Lawrence Berkeley National Laboratory

Lawrence Berkeley National Laboratory

Title

An improved strategy to detect CO2 leakage for verification of geologic carbon sequestration

Permalink

https://escholarship.org/uc/item/5cz867jk

Authors

Lewicki, Jennifer L.
Hilley, George E.
Oldenburg, Curtis M.

Publication Date

2006-05-11

eScholarship.org Powered by the California Digital Library
University of California

An improved strategy to detect surface CO_2 leakage for verification of geologic carbon sequestration

Jennifer L. Lewicki[1], George E. Hilley[2], Curtis M. Oldenburgl[1]

[1]Earth Sciences Division, Lawrence Berkeley National Laboratory,
Berkeley, CA, USA

[2]Department of Geological and Environmental Sciences,
Stanford University, Stanford, CA, USA

Abstract

To detect and quantify subtle surface CO_2 leakage signals, we present a strategy that combines measurements of CO_2 fluxes or concentrations in the near-surface environment with an algorithm that enhances temporally- and spatially-correlated leakage signals while suppressing random background noise. The algorithm consists of a filter that highlights spatial coherence in the leakage signal, and temporal stacking (averaging) that reduces noise from temporally uncorrelated background fluxes/concentrations. We assess the performance of our strategy using synthetic data sets in which the surface leakage signal is either specified directly or calculated using flow and transport simulations of leakage source geometries one might expect to be present at sequestration sites. We estimate the number of measurements required to detect a potential CO_2 leakage signal of given magnitude and area. Results show that given a rigorous field-sampling program, subtle CO_2 leakage may be detected using the algorithm; however, leakage of very limited spatial extent or exceedingly small magnitude may be difficult to detect with a reasonable set of monitoring resources.

Keywords: CO_2, sequestration, leakage, statistics, detection

Introduction

The injection and storage of anthropogenic CO_2 in deep geologic formations is a potentially feasible strategy to mitigate greenhouse gas emissions. While the purpose of geologic carbon sequestration is to trap CO_2 underground, CO_2 could migrate away from the storage site into the shallow subsurface and atmosphere if permeable pathways such as well bores or faults are present. Due to the potentially negative impacts of CO_2 leakage on the sequestration objective and near-surface environment, it is important that storage verification be conducted as an integral part of geologic carbon sequestration. Although a variety of techniques is available to measure near-surface CO_2, leakage detection and storage verification may be challenging due to the large variation in natural background CO_2 fluxes and concentrations, within which a potentially small CO_2 anomaly may be hidden. We present a strategy that combines measurements of CO_2 in the near-surface environment with a statistical algorithm to enhance properties of the data associated with leakage, while reducing random background contributions [1]. Using a suite of synthetic CO_2 flux data sets and simulated CO_2 surface leakage, we investigate combinations of sampling and analysis approaches to optimise leakage detection and quantification while minimizing the number of measurements.

Methods

The statistical algorithm emphasizes two properties of typical natural near-surface CO_2 fluxes and concentrations that contrast from those derived from CO_2 leakage from a storage reservoir. First, the production of CO_2 by background processes (e.g., soil respiration) is highly spatially heterogeneous; resulting soil CO_2 fluxes and concentrations are therefore often poorly correlated on moderate to large spatial scales (e.g., $l \geq 5$ m) [2, 3, 4]. In contrast, CO_2 derived from leakage along a permeable feature such as a well bore or fault should be relatively coherent in space. Second, the production of

background CO_2 is controlled by meteorological and biological processes that operate on diurnal to seasonal time scales and is therefore correlated on these time scales [5, 6, 7, 8]. In contrast, the leakage of CO_2 from a storage reservoir should be relatively constant.

Importantly, the transport of CO_2 from both background sources and leakage will be modified in the near-surface environment by meteorological and biological processes on predictable time scales. Temporal variations in measured soil CO_2 fluxes and concentrations related to these background processes can be removed at predictable wavelengths [4]. Thus, if one measures soil CO_2 fluxes or concentrations in an area in which there may be a small CO_2 leakage signal within background variability, this data can be adjusted to eliminate temporal variability associated with background processes. Areas of elevated spatial and temporal coherence associated with leakage can then be made more obvious.

The algorithm we use to detect and quantify leakage is composed of (1) a filter that highlights spatial coherence in the CO_2 leakage signal, and (2) temporal averaging that reduces noise from temporally uncorrelated background fluxes [1]. To highlight spatial coherence, we progressively move a Gaussian weighting function over a regularly spaced (l = 5 m) grid, and calculate the weighted average of all measured points according to their distance from the specified grid point. This interpolation procedure enhances the spatial correlation of the leakage signal, while decreasing the influence of small-scale variability of background fluxes. To reduce the effect of temporally uncorrelated background noise, we either (1) average repeated measurements at each sampling location, then apply the Gaussian weighting function, or (2) average flux values at each grid point interpolated using the Gaussian weighting function based on repeated measurements at each sample location.

To test different sampling and processing combinations, we created a suite of synthetic data sets in which surface CO_2 leakage was treated as either a two-dimensional scaled Gaussian distribution of surface CO_2 fluxes or was created with a numerical simulator (TOUGH2/T2CA) [9, 10] as the surface CO_2 flux signal associated with leakage along a well bore or a fault. In all cases, background biological noise was added to the surface CO_2 leakage and surrounding area (10^6 m^2, to consider a reservoir-scale area) using a lognormal CO_2 flux distribution measured using the accumulation chamber method [11] in central California [4]. These flux data were adjusted to remove diurnal trends and then the mean, hereafter referred to as F_B, and standard deviation were calculated (= 8.7 and 6.7 g m^{-2} d^{-1}, respectively). Therefore, modeled background fluxes represent the case in which temporal correlation has been removed. To model re-measurement of fluxes over time, a new realization of the background synthetic data set was repeatedly drawn from the distribution and superimposed on the leakage signal and surrounding area.

Using synthetic data sets, we explored a range of sampling and processing strategies. In each, we sampled 100 CO_2 fluxes from the underlying synthetic data set. The strategies included: (1) Sample CO_2 fluxes on a regularly-spaced grid on multiple campaigns, apply Gaussian filtering to each data set, and temporally average fluxes at each interpolated grid point; (2) Randomly sample fluxes in space, repeat sampling at the same locations over time, apply Gaussian filtering to each data set, and temporally average fluxes at each interpolated grid point; (3) Randomly sample fluxes in space and re-randomize locations during each re-sampling, apply Gaussian filtering to each data set, and temporally average fluxes at each interpolated grid point. We assessed the success of each strategy based on the fraction misestimation (f_{ME}) of the total CO_2 leakage rate ($f_{ME} = \sqrt{(\mathrm{ILR} - \mathrm{CLR})^2} / \mathrm{ILR}$), where ILR and CLR are the imposed and calculated leakage rates, respectively (i.e., the spatially integrated leakage flux of the synthetic source).

Results

Strategy three, where fluxes were randomly sampled, and then sample locations were re-randomized during subsequent sampling campaigns, was most successful in consistently detecting and quantifying CO_2 leakage of arbitrary magnitude, area, and location. Figure 1 shows an example of strategy three, and the results shown hereafter are based on implementation of this strategy. We varied the number of repeat sampling campaigns (= 10, 50, 100, 200, and 360) for scaled Gaussian distributions of leakage with R/L = 0.01, 0.1, and 0.5 (R = Gaussian length scale, L = model domain length in x and y directions = 1000 m), while holding F_S/F_B constant (= 1, where F_S is maximum surface CO_2 leakage flux). These R/L values correspond to ratios of the synthetic leakage signal area (A_S) to the total area of the model domain ($A_T = 10^6$ m^2) of 3.14 x 10^{-4}, 3.14 x 10^{-2}, and 0.785. To estimate the distribution of f_{ME} for each case, we performed 100 Monte Carlo realizations of each number of sampling campaigns. Results of repeated sampling campaigns are shown in Figure 2a. We then varied the number of sampling campaigns for F_S/F_B = 0.01, 1, and 100, while holding A_S/A_T constant (=3.14 x 10^{-2}) (Figure 2b). As shown in Figures 1a and b, for a given A_S/A_T or F_S/F_B, f_{ME} decreases non-linearly as the number of sampling campaigns increases, with f_{ME} becoming relatively insensitive to number of sampling campaigns >100. Also, f_{ME} becomes relatively insensitive to the number of sampling campaigns with increasing A_S/A_T or F_S/F_B. For a given number of sampling campaigns, f_{ME} decreases with A_S/A_T or F_S/F_B by up to 2.5 orders of magnitude. However, f_{ME} becomes less sensitive to A_S/A_T or F_S/F_B as A_S/A_T or F_S/F_B increases.

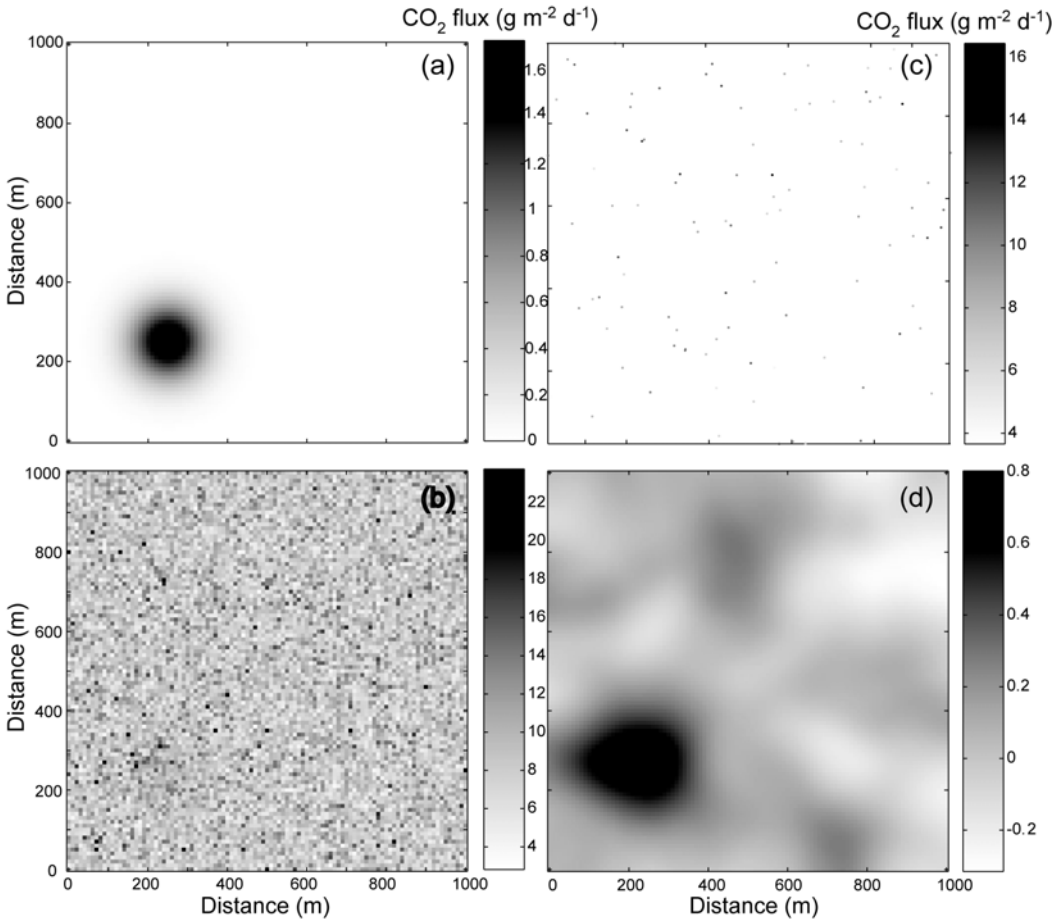

Figure 1 Example of steps in strategy three, 100 repeat sampling campaigns (from [1]). (a) CO_2 leakage signal is a two-dimensional scaled Gaussian distribution. (b) A data set is drawn from the adjusted background distribution and added to the leakage signal and surrounding

areas. (c) One hundred CO_2 fluxes are randomly sampled from (b). Steps (b) and (c) are repeated 100 times in repeated sampling campaigns, re-randomizing the sample locations each time. (d) The Gaussian function filter is applied to each flux sample set and point-by-point averaging is applied to the 100 grids. $f_{ME} = 0.02$ for this example.

To consider more physically realistic cases of CO_2 leakage, we used TOUGH2/T2CA to model two possible leakage scenarios: (1) an abandoned well transports CO_2 from a deep storage reservoir to the vadose zone and (2) a buried fault transports CO_2 to the vadose zone. A CO_2 source was specified in either the fault (linear, 10 x 1000 m) or well (point, 1 x 1 m) geometry at an arbitrary depth of -27.1 m in a three-dimensional vadose zone with surface area = 10^6 m^2. Low, medium, and high source leakage fluxes for the well (3.8 x 10^4, 3.8 x 10^5, and 3.8 x 10^6 g $m^{-2}d^{-1}$, respectively) and fault (3.8, 38, and 380 g $m^{-2}d^{-1}$, respectively) scenarios were chosen to generate F_S values over a range of CO_2 fluxes observed in nature (i.e., from biologic low fluxes to volcanic-magmatic high fluxes), in order to assess a range of f_{ME} values for the two scenarios. The surface leakage fluxes are calculated at $t = 100$ y of model time, at which time they are nearly steady. F_S values corresponding to low, medium, and high leakage fluxes for well simulations are ~16, 160, and 1600 g $m^{-2}d^{-1}$ (F_S/F_B ~1.8, 18.4, 183.9), and for fault simulations are ~0.8, 8, and 80 g $m^{-2}d^{-1}$ (F_S/F_B ~0.09, 0.92, 9.2). As shown in Figure 3, for a given F_S/F_B for both well and fault scenarios, f_{ME} decreases non-linearly with increasing number of sampling campaigns, to become relatively constant at >200 campaigns. However, even though the low, medium, and high F_S/F_B cases for the fault scenario are ~two orders of magnitude lower than those for the well scenario, f_{ME} values are similar. For a given number of sampling campaigns, f_{ME} decreases with increasing F_S/F_B.

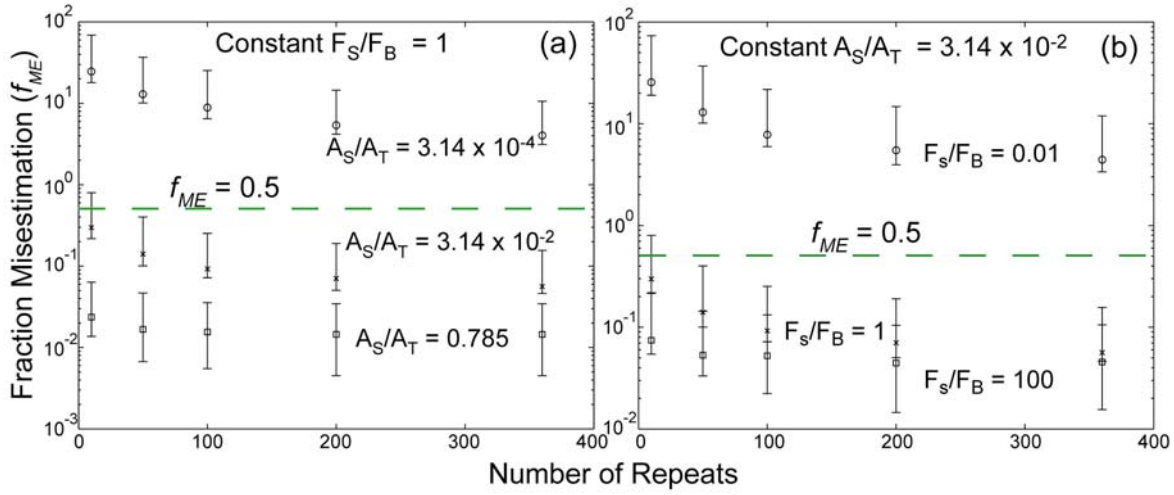

Figure 2 Fraction misestimation (f_{ME}) versus number of repeat sampling campaigns for (a) well and (b) fault scenarios (modified from [1]). The mean and 68% lower and upper bounds of f_{ME}, calculated based on 100 Monte Carlo simulations, are plotted as the symbols and error bars, respectively. Dashed line shows $f_{ME} = 0.5$.

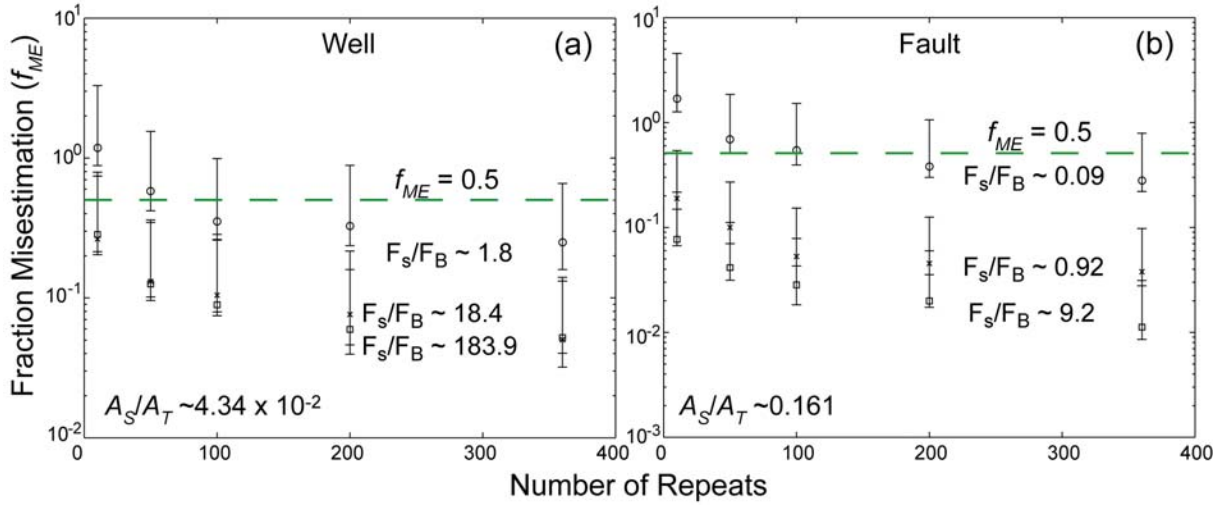

Figure 3 Fraction misestimation (f_{ME}) versus number of repeat sampling campaigns for (a) well and (b) fault scenarios (modified from [1]). The mean and 68% lower and upper bounds of f_{ME}, calculated based on 100 Monte Carlo simulations, are plotted as the symbols and error bars, respectively. Dashed line shows f_{ME} = 0.5.

Discussion and Conclusions

For a given number of sampling campaigns, f_{ME} is sensitive to both the ratio of the maximum leakage flux to the average background flux (F_S/F_B) and the ratio of the synthetic leakage signal area to the total area of the model domain (A_S/A_T). If we conservatively assume that f_{ME} values ≤0.5 represent leakage anomalies detectable within a reasonable error and values >0.5 are "undetectable" anomalies (Figures 2 and 3), we can make the following statements. (1) Leakage with F_S/F_B = 1 is detectable with only 10 sampling campaigns when $A_S/A_T \geq 3.14 \times 10^{-2}$, but for smaller $A_S/A_T = 3.14 \times 10^{-4}$ is undetectable with up to 360 campaigns. (2) Leakage with $A_S/A_T = 3.14 \times 10^{-2}$ is detectable with only 10 sampling campaigns when $F_S/F_B \geq 1$, but for smaller $F_S/F_B = 0.01$ is undetectable with up to 360 campaigns. (3) Simulated surface leakage resulting from CO_2 leakage from a well with $A_S/A_T \sim 4.34 \times 10^{-2}$ and $F_S/F_B \geq 18.4$ is detectable with only 10 sampling campaigns; but leakage with smaller $F_S/F_B = 1.8$ requires at least 100 repeats. (4) Simulated surface leakage resulting from CO_2 leakage from a fault with $A_S/A_T \sim 0.161$ and $F_S/F_B \geq 0.92$ is detectable with only 10 sampling campaigns; but leakage with smaller $F_S/F_B = 0.09$ requires at least 200 repeats.

Due to the relatively high A_S/A_T of simulated leakage anomalies associated with the fault source, it is possible to detect anomalies with low F_S with a reasonable number of samples. This emphasizes the importance of maximizing A_S/A_T in studies where seepage fluxes could have F_S within the background variability of CO_2 flux or could have small A_S (e.g., wells, mostly sealed faults/fractures). We based our example on soil CO_2 flux measurements made using the accumulation chamber method due to its well-tested reliability, the rapidity of each measurement (typically a few minutes), and the availability of a large background CO_2 flux data set collected using this method. However, our method also applies to other gas species (e.g., CH_4) and to subsurface gas concentrations. Due to our ability to rapidly measure soil CO_2 flux or concentration over variable terrain conditions, our example of making 100 measurements within a study area within a given day is reasonable in most circumstances. Therefore, the number of repeat sampling campaigns will equal the number of days required to apply to storage verification. In most cases, 10–50 repeat sampling campaigns should be reasonable within a year; a greater number will depend on available resources.

Our analysis assumes that background CO_2 fluxes and concentrations are statistically uniform over a study area. This may not be the case if there are features such as topography or vegetation that cause relatively consistent CO_2 production over time. To avoid misinterpreting background CO_2 signals in these areas as subtle leakage and distinguish the two sources, physical properties of the study area should be characterized along with soil gas chemical and isotopic analyses. Our method also assumes that CO_2 leakage is slowly evolving over the observation period. If there is interest to detect leakage that is rapidly changing, then additional analysis taking into account a temporally evolving source will be required. In summary, our strategy provides a means to locate and quantify potentially small CO_2 leakage signals derived from geologic storage reservoirs within natural background variability. If leakage is detected, then further geophysical, geochemical, and reservoir management techniques can be applied to locate and mitigate the leak.

Acknowledgements
This work was supported in part by a Cooperative Research and Development Agreement between BP Corporation North America, as part of the CO_2 Capture Project, and the U.S. Department of Energy through the National Energy Technologies Laboratory, and by the Ernest Lawrence Berkeley National Laboratory, managed for the U.S. Department of Energy under Contract No. DE-AC03-76SF00098. We thank A. Cortis (LBNL) for constructive review.

References

- [1] Lewicki JL, Hilley GE, Oldenburg CM. An improved strategy to detect CO_2 leakage for verification of geologic carbon sequestration. Geophys Res Lett 2005; 32 (19): L19403, doi:10.1029/2005GL024281.
- [2] Stoyan H, De-Polli H, Bohm S, Robertson GP, Paul EA. Spatial heterogeneity of soil respiration and related properties at the plant scale. Plant Soil 2000; 222: 203–214.
- [3] Xu M, Qi Y. Soil-surface CO_2 efflux and its spatial and temporal variations in a young ponderosa pine plantation in northern California. Global Change Biol 2001; 74: 667– 677.
- [4] Lewicki JL,Evans WC, Hilley GE, Sorey ML, Rogie JD, Brantley SL. Shallow soil CO_2 flow along the San Andreas and Calaveras faults, CA. J Geophys Res 2003; 108(B4): 2187, doi:10.1029/2002JB002141.
- [5] Buyanovsky GA, Wagner GH. Annual cycles of carbon dioxide level in soil air. Soil Sci Soc Am J 1983; 47: 1139–1145.
- [6] Osozawa S, Hasegawa S. Diel and seasonal changes in carbon dioxide concentration and flux in an andisol. Soil Sci 1995; 160: 117–124.
- [7] Ouyang Y, Zheng C. Surficial processes and CO_2 flux in soil ecosystem. J Hydrol 2000; 234: 54–70.
- [8] Tang J, Baldocchi DD, Qi Y, Xu L. Assessing soil CO_2 efflux using continuous measurements of CO_2 profiles in soils with small solid-state sensors. Agric For Meteorol 2003; 118: 207–220.
- [9] Pruess K, Oldenburg C, Moridis G. TOUGH2 user's guide version 2.0. Rep LBNL-43134, Lawrence Berkeley Natl Lab, Berkeley, Calif., 1999.
- [10] Oldenburg CM, Unger JA. On leakage and seepage from geologic carbon sequestration sites: Unsaturated zone attenuation, Vadose Zone J 2003; 2: 287–296.
- [11] Norman JM, Garcia R, Verma SB. Soil surface CO_2 fluxes and the carbon budget of a grassland. J Geophys Res 1992; 97: 18,845–18,853.